Diabetes, Metabolic Syndrome and Obesity: Targets and Therapy Dovepress
open access to scientific and medical research

Open Access Full Text Article

ORIGINAL RESEARCH

Eight Differential miRNAs in DN Identified by Microarray Analysis as Novel Biomarkers

Chao Tu[1], Lan Wei[1], Liangzhi Wang[1], Ying Tang[2]

[1]Department of Internal Medicine, The Third Affiliated Hospital of Soochow University, Changzhou, Jiangsu, People's Republic of China; [2]Department of Rehabilitation Medicine, The Third Affiliated Hospital of Soochow University, Changzhou, Jiangsu, 213000, People's Republic of China

Correspondence: Ying Tang, Department of Rehabilitation Medicine, The Third Affiliated Hospital of Soochow University, 185 Juqian Road, Changzhou, Jiangsu, 213000, People's Republic of China, Tel +86 0519 68872146, Email tyczfph@yeah.net

Background: Diabetic nephropathy (DN) is the common cause of renal diseases such as end-stage renal disease (ESRD) and chronic kidney disease (CKD). Various diagnostic applications and treatment methods are used for clinical but remain some prognosis issues. To avoid morbidity and mortality related to DN, early detection of disease complications as well as targeted therapeutic strategies is essential. Considerable evidence indicates that non-coding RNA plays a vital role in the biological processes of various diseases, used as biomarkers and therapeutic targets. And the most known ncRNAs are the microRNAs (miRNAs), long noncoding RNAs (lncRNAs), and circular RNAs (circRNAs).

Materials and Methods: Our study aimed to identify potential prognostic ncRNAs involved in DN by bioinformatics analysis and validated expression levels through quantitative polymerase chain reaction (qPCR) and GEO database. Our research focuses on differential expression miRNAs (DEmiRNAs) in DN and their interactions with critical genes.

Results: We identified 8 up-regulated DEmiRNAs, including miR-103a-2-5p, miR-297, miR-548x-3p, miR-604, miR-644a, miR-1256, miR-3911 and miR-5047 finally. We further validated these miRNAs in a murine model.

Conclusion: Identifying these up-regulated genes and elucidating these miRNAs regulatory network will contribute to a better understanding of the molecular mechanism of DN and how they can be used as new biomarkers and potential therapeutic targets for DN.

Keywords: diabetic nephropathy, microRNAs, bioinformatics, biomarkers

Introduction

By 2045, it is estimated that there will be 693 million diabetic patients of the world.[1] Diabetic nephropathy (DN) is the main complication of diabetes mellitus (DM), also is one of the most severe microvascular complications, more than 40% of diabetes patients are affected by it.[2] The main pathological features of DN include glomerular hypertrophy, proteinuria, decreased glomerular filtration rate and renal fibrosis.[3] In recent years, urinary albumin excretion rate (UAER) acts as an early biomarker of DN, kidney injury molecule-1 (KIM-1) is widely studied as a diagnostic marker.[4] The current treatment strategies for DN are mainly to control blood sugar and blood pressure levels, in the meantime inhibit the renin-angiotensin (RAS) system to reduce proteinuria and delay the development of DN.[5] Considering the high incidence of end-stage renal disease associated with DN, the treatment effect is not completely satisfactory. Therefore, there is an urgent need to determine new treatment goals.

Non-coding RNA (ncRNA) inhibits the translation or degradation of target messenger RNA (mRNA) by inhibiting RNA interference and becomes a regulator of gene expression modification, which has attracted attention and research.[6] Most of these ncRNAs are generally grouped based on their sizes, which are the small ncRNAs (< 200 nucleotides) that include the microRNAs (miRNAs) and some of the circular RNAs (circRNAs) and the large ncRNAs such as the long ncRNAs (lncRNAs).[7] A large number of research results reveal the role of miRNA in the occurrence and development of various diseases including diabetic nephropathy. At the same time, changes in miRNA levels can be used not only as diagnostic biomarkers but also as therapeutic targets for cancer and certain inflammatory diseases.[8] Multiple studies have

Received: 25 December 2021
Accepted: 11 March 2022
Published: 24 March 2022

Graphical Abstract

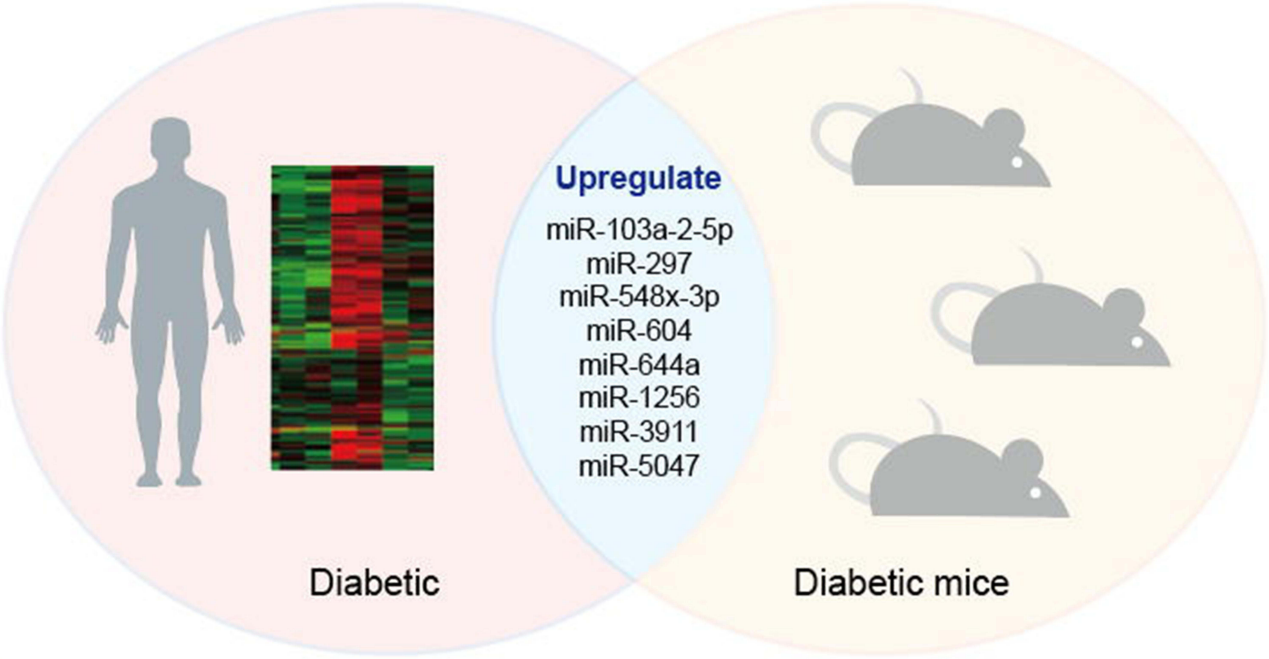

confirmed that miRNAs play a key role in the occurrence and development of diabetic nephropathy and may represent potential biomarkers and treatment options for diabetic nephropathy.[9,10]

High-throughput sequencing technology provides an efficient method for studying disease related genes and provides promising drug targets in many fields. So far, several studies have screened genes or miRNAs related to DN.[11,12] Our study identified target genes that may enhance the understanding of the molecular mechanism of DN, proved the role of several miRNAs in DN through animal experiments, the target gene network associated with these miRNAs was established at the same time. These results provided new targets and directions for further follow-up research.

Materials and Methods

Gene Expression Profiles Data

We downloaded the GSE96804 dataset from the GEO database (http://www.ncbi.nlm.nih.gov/geo).[13] The expression profiling arrays of GSE96804 were generated using GPL17586 [HTA-2_0] Affymetrix Human Transcriptome Array 2.0 [transcript (gene) version], including 41 patients with type 2 DM confirmed by renal biopsy and 20 healthy control glomerular samples from unaffected portion of tumor nephrectomies, and preprocessed using a gene-level (RMA-Sketch) workflow. In the quality control step of the workflow, all samples are determined to be of high quality. Kidney samples were taken from the remaining part of surgical nephrectomy and diagnostic renal biopsy. All procedures performed in this study were in accordance with the ethical standards of the institutional and/or national research committee and with the Helsinki Declaration (as revised in 2013). The raw data were read by the GEO2R tool as well as normalized and $\log_2$-transformed data. Then, the edgeR package in R[14] was used to identify DECs in GSE96804 dataset with the standard of |log2 (fold-change)|<0.5 and > 2, adjusted p-value <0.01. In addition, the corplot_heatmap and scatter plot were output using R software.

Construction of miRNA-DEG Regulatory Network

Through 5 databases miRWalk, miRanda, miRDB, RNA22 and Targetscan to predict microRNA target genes, and screen out the target mRNAs supported by the 3 databases at least. Differential expression target genes (DEtmRNAs) were obtained by the intersection of the target gene and differential gene. The regulatory network consisting of DEGs and miRNAs were visualized by Cytoscape (http://cytoscape.org/).[15]

Enrichment Analysis by Metascape

Gene Ontology (GO), Kyoto Encyclopedia of Genes and Genomes (KEGG), and transcription factor (TF) analysis were conducted and visualized by metascape (http://metascape.org/). The parameters were set as defaulted.

Murine Model

Six-weeks-old, C57BL/KsJdb/db diabetic and nondiabetic littermate control db/m mice (Male, 20–25 g, 8 weeks old) were housed in a pathogen-free cage at a constant temperature of 22±2°C and humidity of 50±5%, with normal air CO_2 levels, 12 h light/dark cycles and ad libitum access to standard diet and water. Measuring the body weights of mice at 8, 16, and 22 weeks of age. During the experiment, the fasting blood glucose (FBG) and random blood glucose (RBG) were measured at 8, 16, and 22 weeks. Finally, collect the urine of mice at 22 weeks for urine protein/creatinine detection. We selected 5 db/db mice and 5 db/m mice as experimental verification, and each mouse made 3 biological replicates. The animal experiments were conducted following the standard for laboratory animals of the Third Affiliated Hospital of Soochow University.

Histological Examination

The kidney tissues of mice in each group were fixed, dehydrated, embedded in paraffin, and cut into 5 μm slices. The slices were deparaffinated, rehydrated, and then subjected to routine hematoxylin-eosin (HE) staining and Masson's trichrome staining. HE staining was performed as follows: the renal cortex was baked at 60°C and then dewaxed with xylene I, xylene II and xylene III; the tissue was dehydrated in 100%, 90%, 80%, and 70% ethanol solution; incubate tissue in distilled water for 5 minutes to complete rehydration; the slices were stained in hematoxylin aqueous solution (Beyotime, China) for 5 minutes, rinsed in distilled water, and treated with 0.1% HCl/ethanol differentiation; the tissues were stained in eosin (BBI Life Sciences, China) for 3 minutes, rinsed in tap water for 5 minutes; the slices were baked and dehydrated with ethanol again; and after transparent treatment with toluene, the film was sealed with neutral gum and imaged under the optical microscope. Dewaxing, sealing, and HCl/ethanol differentiation of Masson's trichrome staining are the same as HE staining, Masson dye kit (Servicebio, China) was used for dyeing, glacial acetic acid was used for rinsing differentiation, anhydrous ethanol was used for dehydration. Images were captured under a microscope (IX71, OLYMPUS, Tokyo, Japan).

Quantitative Real-Time PCR

RNA was extracted from frozen kidney cortex tissues using QIAzol Lysis Reagent according to the manufacturer's instructions (Ambion, USA). We use A260/280 of 1.8–2.0 to be the criteria to check RNA quality. Then, the total RNA was converted to complementary deoxyribonucleic acid (cDNA) using a reverse transcription reagent kit (Thermo, USA). Quantitative real-time polymerase chain reaction (qRT-PCR) was performed with SYBR Green PCR reagent (Thermo, USA) for quantification of the miRNA levels. Calculations were made based on the comparative cycle threshold method ($2^{-\Delta\Delta Ct}$).[16] The $2^{-\Delta\Delta Ct}$ method was used to compare the relative expression levels in the experimental group compared with the control group. The control group was used as the calibrator group and U6 was used as an endogenous normalization control. Primer sequences are given in Table 1.

Statistical Analysis

GraphPad Prism version 7 (GraphPad software) was used for all statistical analysis. The results of qRT-PCR were shown as mean ± Standard Error of Mean (SEM). Other data were expressed as mean ± standard deviation (x ± SD). The differences between the two groups were compared using the unpaired Student's *t*-test, where the differences among

Table 1 Sequence of Primers for Quantitative Real-Time PCR

Gene	Forward Primer	Reverse Primer
miR-103a-2-5p	GAGCAGCATTGTACAG	GTGCAGGGTCCGAGGT
miR-297	ACGCTCAGTTAATGCTAATCGTGATA	ATTCCATGTTGTCCACTGTCTCTG
miR-548x-3p	TAAAAACTGCAATTACTTTC	CTCAACTGGTGTCGTGGAGTCGGCAATTCAGTTGAGTGAAAG
miR-644a	AGTGTGGCTTTCTTAGAGC	CTCAACTGGTGTCGTGGAGTCGGCAATTCAGTTGAGATCTCG
miR-604	AGGCTGCGGAATTCAGGAC	CTCAACTGGTGTCGTGGAGTCGGCAATTCAGTTGAGGTCCTG
miR-1256	GGCGCGATTTTAGTTTATC	TTTAATTACCAACCGAATACG
miR-3911	TGTGTGGATCCTGGAGGAGGCA	CTCAACTGGTGTCGTGGAGTCGGCAATTCAGTTGAGCTCCGT
miR-5047	GCCTAGACGAGACACAGTGC	GCCAAGACCTTACAACCGCA
U6	CTCGCTTCGGCAGCACATATACTA	ACGAATTTGCGTGTCATCCTTGCG

more than two groups were evaluated using the one-way ANOVA followed by Turkey's multiple comparisons test. Statistically significance was set at *$p< 0.05$, **$p< 0.01$ and ***$p< 0.001$.

Results

Differentially Expressed Diabetes Nephropathy Related RNAs

To identify essential mRNAs and ncRNAs in DN, raw microarray data were downloaded from GEO (dataset no. GSE96804). To obtain differentially expressed RNAs, the signal data were normalized and z-score-transformed (unpaired *t*-test according to the experimental design was used to validate statistical significance). The analysis results were visualized by heatmap (Figure 1A and C). It was determined that numerous mRNAs and ncRNAs were differentially expressed in patients with DN compared to normal controls. Similarly, we also described the DEmRNAs and DEncRNAs of the dataset in the form of volcano plots (Figure 1B and D).

Next, research focus on the differential expression of miRNAs in non-coding RNA. In GSE96804, we identified 54 differentially expressed miRNAs in DN tissue specimens compared with normal tissue specimens, including 53 up-regulated genes and 1 down-regulated gene (Table 2). We selected 8 miRNAs that were differentially expressed in Type 2 DM and poorly studied in DN for further detailed expression heatmap (Figure 1E).

Establishment of Animal Model for DEmiRNAs and DEmRNAs Validation

In order to identify the correlation between 8 up-regulated miRNAs and DN, we used mice model to verify it. Weight, FBG and RBG are related to diabetes, we test these at 8, 16 and 22 weeks. It can be seen that compared with the control group, three indicators of the DN mice changed significantly for three measurements (Figure 2A–C). The continuous monitoring data of FBG and RBG showed that DN mice had diabetic symptoms (RBG greater than 16.7 mmol/L is the criterion for successful modeling). In the meantime, results of urinary albumin/creatinine ratio at 22 weeks showed significant difference between DN and control group (Figure 2D). In addition, picture of HE staining showed that compared with the control group, the glomerular capillary lumen of DN group was hyaline, there were inflammatory cells infiltration in renal interstitium, and the renal tubular basement membrane was thickened, but there was no significant difference between the groups. However, Masson staining showed that the collagen production in the kidney of DN group increased gradually (shown in blue), and the degree of lesion was obvious (Figure 2E). All about these indicated that the diabetic nephropathy model has been successfully constructed and the condition is stable, mice model can be used to study the expression of miRNA.

Expression Levels of DEmiRNAs in Mice Model

In order to verify whether the expression of DEmiRNAs were consistent with the analysis results, we used qRT-PCR technology to text the expression of miRNA in mice renal cortex. The results showed that compared with the control group, miR-103a-2-5p, miR-297, miR-548x-3p, miR-604, miR-644a, miR-1256, miR-3911 and miR-5047 were significantly up-regulated, which were constant with the chip data set GSE96804 results (Figure 3).

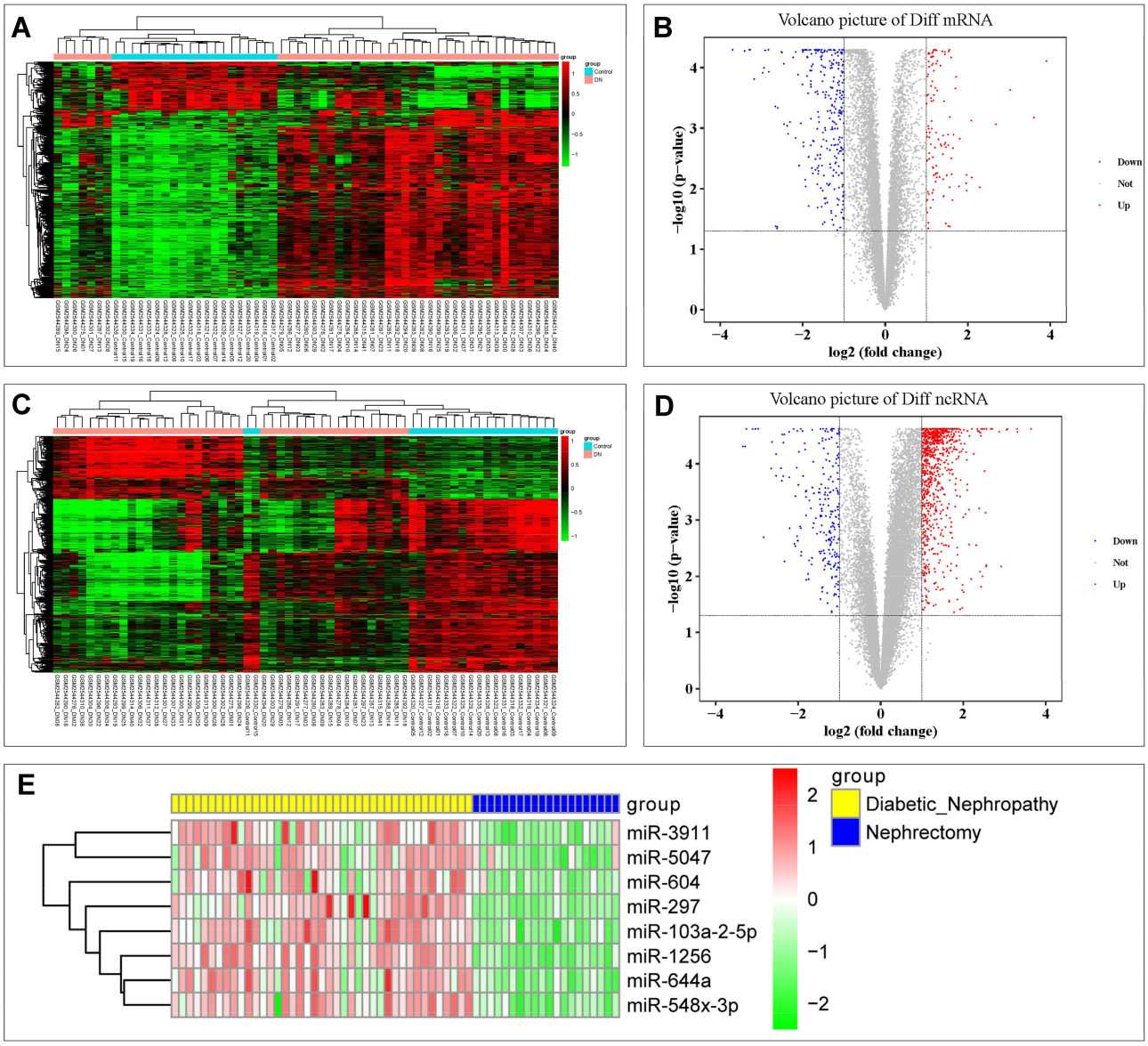

Figure 1 Expression profiling of mRNA and ncRNA in Diabetes Nephropathy. The heat map reveals the different levels of expression of each mRNA (**A**) or ncRNA (**C**) from high to low, represented by green to red squares. Pink represents DN group and blue represents control group. Volcano plots demonstrated the differentially expression levels in DN and control group. Red dots and green dots represent the significantly upregulated and downregulated mRNAs (**B**) or ncRNA (**D**) (FC ≥2.0 and p-value <0.05). (**E**) Heatmap of 8 differentially expressed miRNAs. The dark blue represents the nephrectomy group and the yellow represents the diabetic nephropathy group.

Prediction of Target Genes for the miRNAs

To further predict the targets genes of miR-103a-2-5p-5p, miR-297, miR-548x-3p, miR-604, miR-644a, miR-1256, miR-3911 and miR-5047, the online target prediction analysis tools including miRwalk, TargetScan and miRanda were utilized. Differential expression target genes were obtained by the intersection of the target gene and differential gene. A total of 233 target genes were screened out for the 8 miRNAs with 3 bioinformation database. The interaction network between 8 DEmiRNAs and the corresponding mRNAs were visualized by Cytoscape (Figure 4).

Enrichment Analysis

In order to study the functions of 8 DEmiRNAs and target genes in DN, we conducted enrichment analysis. Gene ontology enrichment analysis divides the functions of genes into three parts: biological process (BP), Cellular Component (CC) and

Table 2 Differential Expression miRNAs of DNin GSE96804

Gene Symbol	Style	Fold Change	p-value
MiR-1254-1	Up	3.02247	0.000024
MiR-1256	Up	3.285812	0.000024
MiR-4256	Up	6.37481	0.000024
MiR-4521	Up	9.923141	0.000024
MiR-548AD	Up	2.788169	0.000024
MiR-548D-1	Up	2.407419	0.000024
MiR-548D-2	Up	2.93304	0.000024
MiR-548F-1	Up	2.68418	0.000024
MiR-548G	Up	2.661163	0.000024
MiR-297	Up	3.018371	0.000025
MiR-548AI	Up	2.725295	0.000025
MiR-548AJ-2	Up	2.540173	0.000025
MiR-548O-2	Up	3.343645	0.000025
MiR-548A-3	Up	2.997301	0.000026
MiR-548Q	Up	2.811621	0.000026
MiR-4454	Up	2.719549	0.000027
MiR-548AA-2	Up	2.847249	0.000027
MiR-103A-2-5p	Up	3.121686	0.000028
MiR-1285-2	Up	2.204645	0.000028
MiR-30A	Up	2.38041	0.00003
MiR-548T	Up	3.280625	0.00003
MiR-644A	Up	3.396481	0.000033
MiR-103B-2	Up	3.016734	0.000035
MiR-503	Up	2.620423	0.000037
MiR-450B	Up	2.769367	0.000038
MiR-548H-3	Up	2.608557	0.000039
MiR-548X	Up	3.562086	0.00004
MiR-548H-2	Up	3.047273	0.000043
MiR-548AC	Up	2.283051	0.000052
MiR-548H-4	Up	2.197702	0.000052
MiR-548C	Up	2.123622	0.000053
MiR-548F-3	Up	2.318714	0.000057
MiR-548AN	Up	2.28931	0.000073
MiR-5047	Up	3.722067	0.000074
MiR-3911	Up	3.563088	0.000083
MiR-548W	Up	2.939164	0.000094
MiR-3671	Up	2.20647	0.000134
MiR-1299	Up	2.343402	0.000193
MiR-3120	Up	2.298973	0.00021
MiR-570	Up	2.31557	0.00021
MiR-612	Up	2.570126	0.000251
MiR-186	Up	2.213134	0.000283
MiR-604	Up	4.296393	0.000296
MiR-30E	Up	2.127547	0.000315
MiR-548K	Up	2.425764	0.000337
MiR-548A-2	Up	2.899226	0.000347
MiR-95	Up	2.466617	0.000391
MiR-421	Up	2.635696	0.000402
MiR-3916	Up	2.723917	0.000775
MiR-4263	Up	2.05791	0.001236
MiR-3975	Up	2.975744	0.001336
MiR-4275	Up	2.076779	0.005979
MiR-548I-4	Up	2.259291	0.008164
MiR-614	Down	−2.154721	0.015345

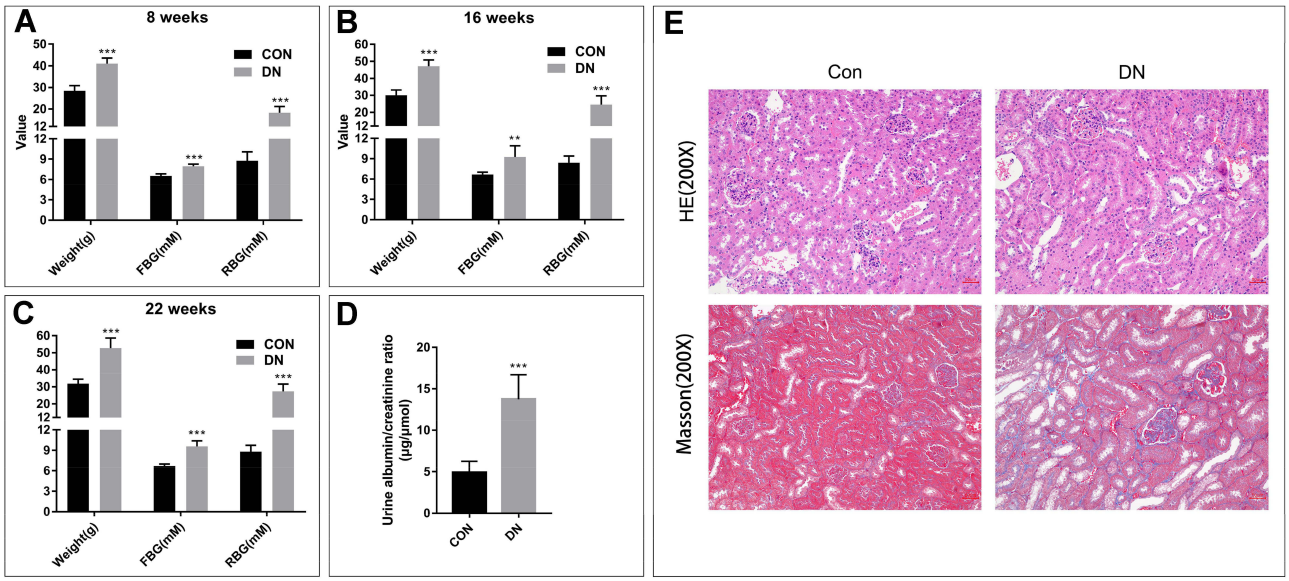

Figure 2 Establishment of DN animal model. (**A**–**C**) Weight, FBG and RBG of mice model at 8, 16 and 22 weeks. (**D**) Urinary albumin/creatinine ratio at 22 weeks in mice model. (**E**) HE and Masson staining of kidney of mice. The number of mice in each group was 5. (**P<0.01, and ***P<0.001).

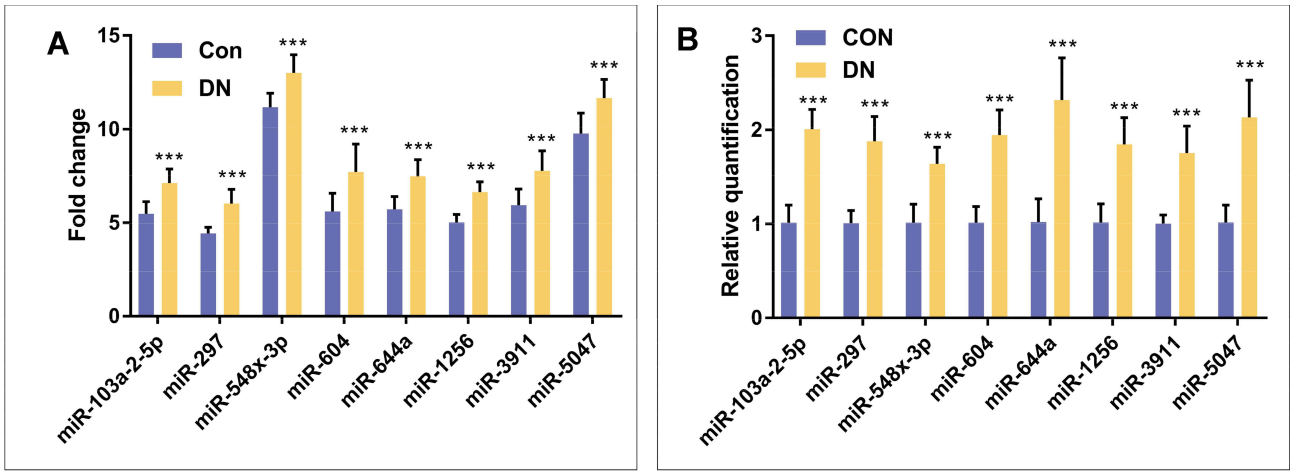

Figure 3 Expression levels of 8 DEmiRNA. (**A**) The difference between DN group and control group of miR-103a-2-5p, miR-297, miR-548x-3p, miR-604, miR-644a, miR-1256, miR-3911 and miR-5047 in the chip data set GSE96804. (**B**) Verification of DEmiRNAs expression by qRT-PCR in mice model. (***P<0.001).

molecular function (MF). As can be seen from the figure of enrichment terms of each input gene, the top 3 highest enrichment degree of GO in the BPareglucose metabolic process, angiogenesis and negative regulation of transcription by RNA polymerase II (Figure 5A). The top 3 highest enrichment degree of GO in the CC are extracellular exosome, plasma membrane and integral component of plasma membrane (Figure 5B). The top 3 highest enrichment degree of GO in the MF are protein binding, protein homodimerization activity and metal ion binding (Figure 5C). In order to further study the relationship between target genes, we conducted pathway analysis. We found that the top 3 significant pathways in the analysis are metabolic pathways, Hippo signaling pathways and protein digestion and absorption pathways (Figure 5D).

Multiple Relationship of Real-Time Quantitative PCR for 8 Differential miRNAs

In miR-3911, the average RQ of the control group was 1.006 and that of the experimental group was 1.500. In miR-5047, the average RQ of the control group was 1.017 and that of the experimental group was 1.250. In miR-1256, the average

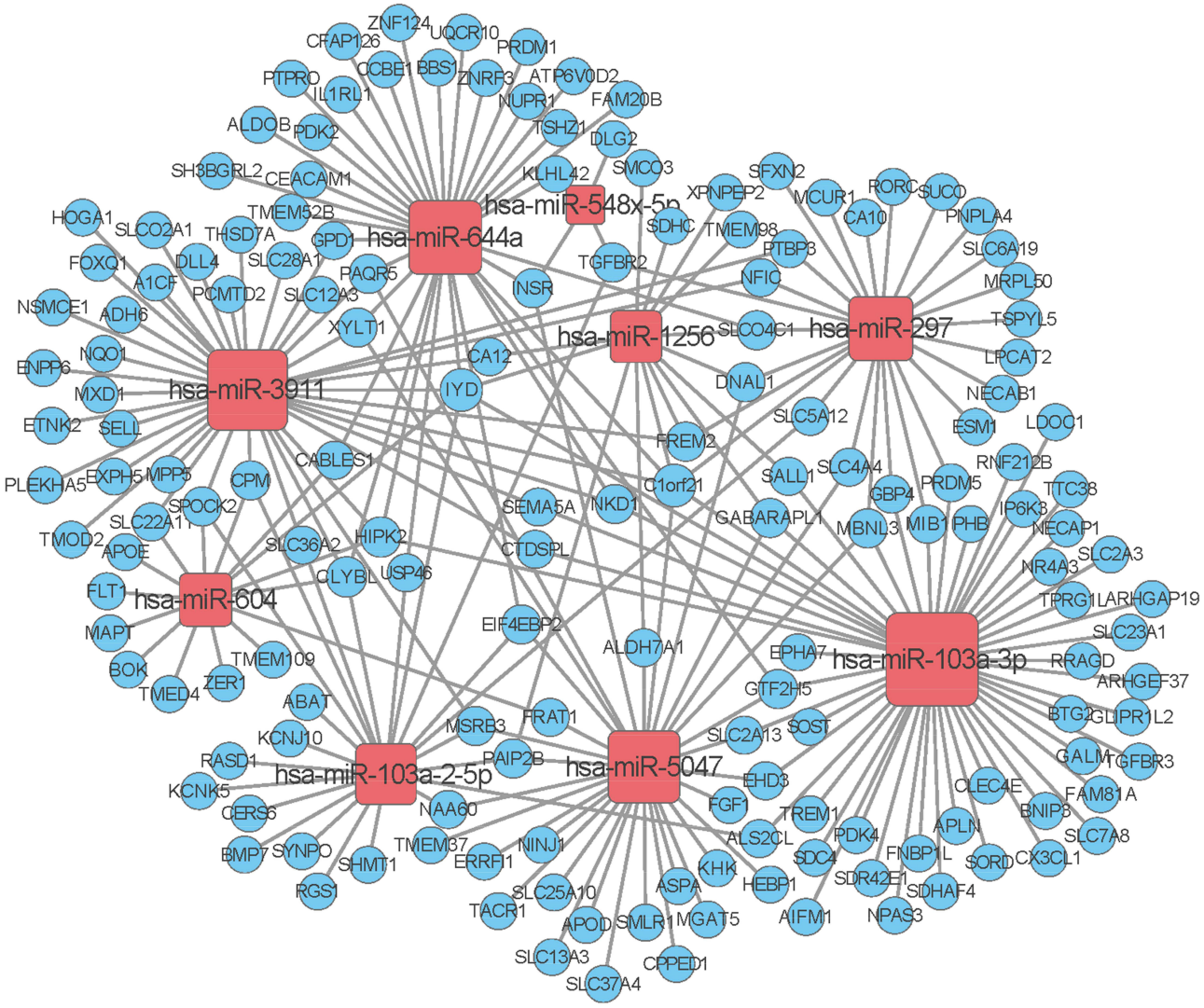

Figure 4 Interaction network of 8 verified DEmiRNAs represented by red and their target DEmRNAs represented by yellow.

RQ of the control group was 1.007 and that of the experimental group was 2.198. In miR-644a, the average RQ of the control group was 1.004 and that of the experimental group was 1.751. In miR-604, the average RQ of the control group was 1.007 and that of the experimental group was 1.722. In miR548x-3p, the average RQ of the control group was 1.015 and that of the experimental group was 1.901. In miR-297, the average RQ of the control group was 1.011 and that of the experimental group was 1.667. In miR-103a-2-5p-5p, the average RQ of the control group was 1.006 and that of the experimental group was 1.931. The above trends are consistent with the results of the chip data.

Discussion

In previous studies, due to the regulation of key genes by various miRNAs in disease process, a variety of miRNAs related to diabetic nephropathy have been discovered. At the same time, GSE databases based on gene chip technology are usually used to detect differentially expressed genes in diseases, provide high-throughput data for genetic research, and obtain differentially expressed genes. Thereby, providing a solution for finding possible differentially expressed genes, which related to diabetes nephropathy.

In this study, gene expression profiles GSE96804 containing 41 cortexes of kidney and matched normal kidney tissues were analyzed. Based on those bioinformatics technologies, we reanalyzed and discovered coding RNAs and non-coding RNAs that are differentially expressed in patients with Type 2 DMvs normal group. After screening out 58 differential

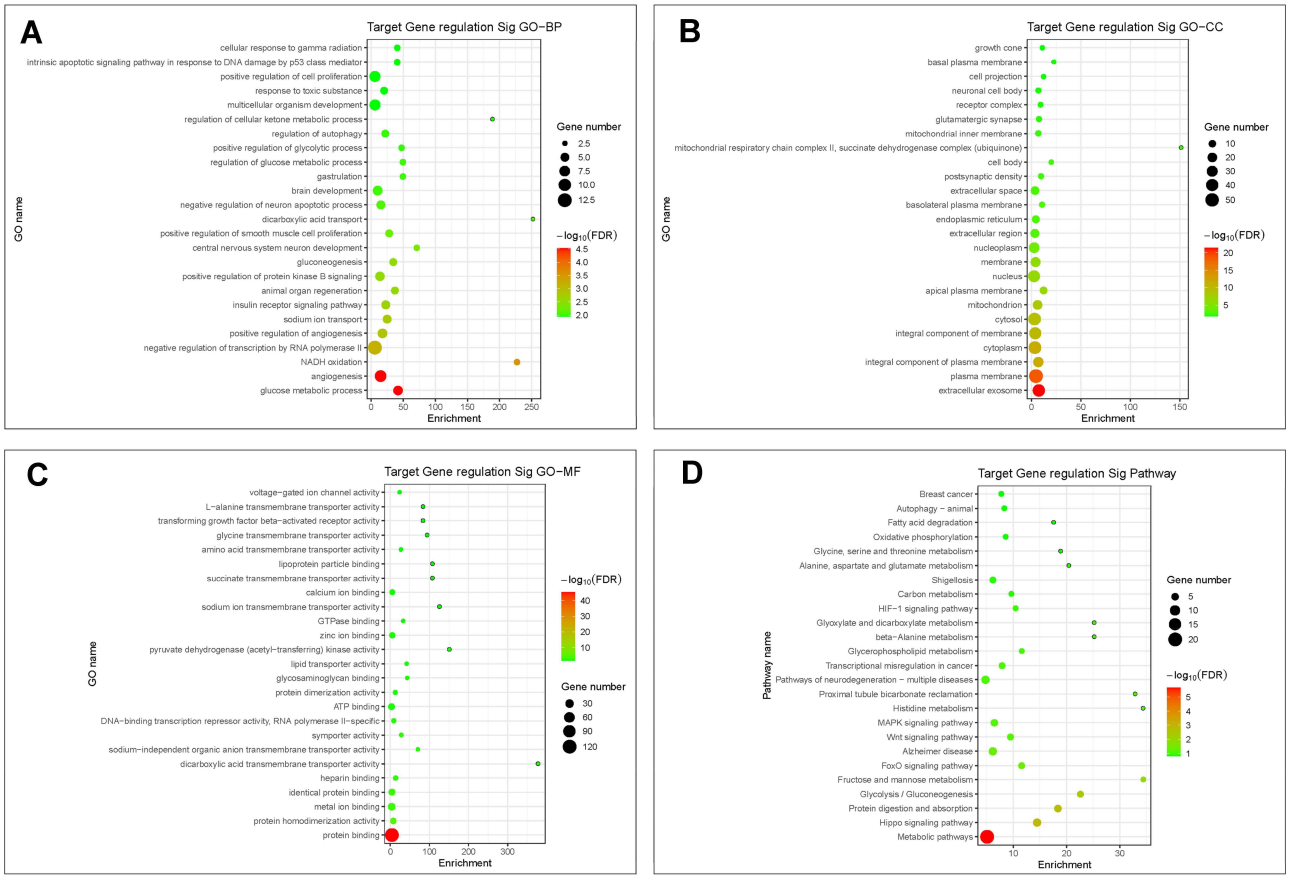

Figure 5 GO enrichment analysis of 8 DEmiRNAs and target genes. (**A**–**C**) The top 25 GO terms for BP, CC and MF. (**D**) The top 25 differential enrichment pathway analysis of target genes. Their enrichment score (FDR of -log10) is indicated from green to red. The size of the dot represents the degree of enrichment, with large dot representing high degrees of enrichment.

expression miRNAs, we continued to use the mouse model to verify the up-regulated genes. Some DEmiRNAs have been already studied about their function in some diseases or cancers for several years. For instance, miR-95 could be important for acute myeloid leukemia prognosis,[17] also loss-of-function assays suggested that miR-95 could function as a tumor promoter by directly binding to its downstream target gene to influence prostate cancer,[18] and miR-95-mediated effects on osteosarcoma tumor growth.[19] Another example is miR-612 binding multiple targeting lncRNA to affect the migration and apoptosis of cancer cells like gastric cancer,[20] bladder carcinoma,[21] cholangiocarcinoma,[22] hepatocellular carcinoma et al[23] MiR-570 plays an important role in the proliferation and immune escape of hepatocellular carcinoma,[24] it also directly targeted IRS1 and IRS2 in chronic myelogenous leukemia to suppressing cell proliferation and glucose metabolism.[25] Moreover, the miR-421 plays an important role in the development and progression of ovarian cancer cells,[26] also play an anti-apoptotic role in colorectal cancer. There have been many related studies on miR-503, silencing of miR-503 in mesenchymal stem cells exerts potent antitumorigenic effects in lung cancer cells,[27] and it could participate high-glucose-induced proximal tubular cell apoptosis, providing a new target for diabetic nephropathy treatment.[28] We selected 8 up-regulated miRNAs in the DN.

In the mice model, we verified miR-103a-2-5p, miR-297, miR-548x-3p, miR-604, miR-644a, miR-1256, miR-3911 and miR-5047 are up-regulated in db/db mice cortex of the kidney. Except for miR-103a-2-5p, other up-regulated miRNAs all play a role in various diseases at present. Details of 8 miRNAs expression on different diseases were list in Table 3. Recently evidence suggests that the expression of miR-297 is frequently altered in many tumors and inflammatory diseases, such as acute myocardial ischemia, bacterial infections or some cancers; research found miR-548x-3p could play a potential role as a modulator of the bone remodeling process. MiR-604 significantly associated with recurrent implantation failure, which defined when pregnancy failure occurs after two consecutive in vitro fertilization-

Table 3 Effects of Changes of miRNA Expression Levels on Disease

miRNAs	Binding Target	Impact on Disease
miR-103a-2-5p	/	/
miR-297	hsa_circ_0007623	Acute myocardial ischemia[46]
	CDK8	Lung cancer[47]
	LINC00668	Oral squamous cell carcinoma[48]
	MRP-2	Colorectal cancer[49]
miR-548x	STAT1, MAFB	Bone remodeling[50]
miR-604	/	Liver cancer and HBV infection[51]
miR-644a	BCAR4	Bladder cancer[52]
	Heat shock factor 1 (HSF1)	Hepatocellular carcinoma[53]
	MEG3	Osteosarcoma[54]
	Carboxyl-terminal-binding protein 1 (CtBP1)	Gastric cancer[55]
	PITX2	Esophageal squamous cell carcinoma[56]
miR-1256	LINC00691	Osteosarcoma[57]
	5-hydroxy tryptamine receptor 3A	Papillary thyroid cancer[58]
	circHECTD1, circ-DCAF6	Gastric cancer[59,60]
	circ_0026134, TCTN1	Non-small cell lung cancer[61,62]
	/	Colorectal cancer[63]
	/	Prostate cancer[64]
miR-3911	/	Human endothelial progenitor cells Regeneration[65]
	/	Autosomal dominant polycystic kidney disease[66]
miR-5047	NEAT1	Parkinson's disease[67]
	LINC01207	Head and neck squamous cell carcinoma[68]
	hsa_circ_0023404	Cervical cancer[69]

embryo transfers to the endometrium using at least four high-quality embryos in women; meantime miR-644a was identified as a tumor suppressor miRNA previously that inhibited oesophageal cancer cell proliferation, also inhibited breast cancer cell proliferation and drug resistance; miR-1256 located in 1p36.12, reported to be dysregulated in prostate cancer firstly; although the mechanism underlying proangiogenic function of brain-derived neurotrophic factor (BDNF) is not fully cleared, some evidences showed miR-3911 might down-regulated because of BDNF. Those up-regulated miRNAs are more or less associated with certain diseases, most of them have their own binding target and studied as a molecular target in many diseases.

Podocytes are highly differentiated glomerular epithelial cells attached to the outer surface of the renal basement membrane and play a key role in maintaining the integrity of the glomerular filtration barrier. Podocyte injury can lead to albuminuria, accumulation of extracellular matrix and glomerulosclerosis, so podocyte injury plays an important role in the occurrence and development of DN.[29] As a basic regulator of gene expression, MiRNAs plays an important role in the occurrence and development of DN. It is mainly involved in various biological processes of podocyte injury, such as apoptosis, fibrosis, inflammation, migration and proliferation.[9] It has been reported that the expression levels of many miRNAs in podocytes in DN mouse model changed under the stimulation of high concentration of glucose.[30] Wang et al[31] found that high glucose stimulation could inhibit podocyte apoptosis and reduce the occurrence of diabetic nephropathy by increasing the expression of target mRNA sirtuin7 of miRNA-20b. MiRNA-21 has been shown to decrease the expression of endorphins and increase the expression of TGF-SMA in cultured mouse podocytes by activating α-catenin and β-β1/Smads pathways.[32] In addition, Loboda et al[33] found that TGF-β can up-regulate the expression of miR-21 in vascular endothelial cells and participate in the tissue fibrosis induced by TGF-β, which leads to renal fibrosis. Chen et al[34] reported that in streptozotocin-induced DN rats, KD with its specific inhibitor miRNA-21 decreased the expression of proinflammatory cytokines such as interleukin-1 β and tumor necrosis factor-α, and alleviated renal damage.[35] It is suggested that the up-regulation of renal miR-21 is positively correlated with the severity of renal injury, renal fibrosis and renal dysfunction, and the application of miRNA-21 inhibitors may be a strategy for the treatment of DN.[36] The protective effect of MiRNA-23b on DN may be achieved by

activating p38MAPK to inhibit the production of extracellular matrix proteins in DN, Zhao et al[37] found that intravenous injection of miR-23b inhibitor could inhibit the expression of miRNA-23b in kidney and increase renal fibrosis, podocyte apoptosis and proteinuria in mice. These results suggest that miRNA-23b has a protective effect on podocyte injury in diabetic nephropathy. MiRNA-27a can reduce the injury of podocytes, including the apoptosis of podocytes and the level of migration and invasion of stimulated podocytes. The specific mechanism is to reduce proliferator-activated receptor gamma (PPAR- γ) and activated β-catenin, thereby reducing epithelial-mesenchymal transformation and podocyte apoptosis.[38] MiRNA-29a has been shown to reduce the apoptosis of podocytes stimulated by high glucose concentration. The specific mechanism is to improve the integrity of podocytes by reducing the deacetylation and ubiquitin-dependent brain peptide deacetylation of histone deacetylase.[39] Overexpression of miRNA29a can inhibit the production of type I and III collagen in renal tubular epithelial cells mediated by transforming growth factor β, and reduce the formation of fibrosis.[40] Xiao et al[41] showed that miR-29a knockout db/db mice reduced proteinuria by inhibiting apoptosis, glomerular Mesangial matrix accumulation and type IV collagen expression. MiR-192 is highly expressed in glomeruli, podocytes and renal endothelial cells of diabetic db/db mice. MiR-192 increases the expression of transforming growth factor-β 1 through Smad3 self-regulation, which promotes the formation of renal fibrosis, suggesting that miR-192 plays an important role in the expression of extracellular matrix genes associated with DN.[42] MiRNA-874 enhanced the survival and proliferation of mouse podocytes stimulated by high glucose by inhibiting the expression of target mRNAToll-like receptor 4 (TLR4) of miRNA-874 in vitro. TLR4 can promote the expression of interleukin-6 (IL-6), tumor necrosis factor-α (TNF–α) and interleukin-1 (IL-1) β. MiRNA874 can inhibit the expression of TLR4 and reduce inflammation, thus reducing proteinuria and delaying the progression of renal function.[43] There are also some miRNA negative regulators of transforming growth factor-β1 signal pathway, including miR141, miR-200a and miR-30c, which can be used as miRNA to inhibit the formation of DN.[44] For example, miRNA141 and miRNA-200a can reduce renal fibrosis by negatively regulating transforming growth factor-β2. In addition, miR-141 down-regulates the expression of transforming growth factor-HIPK1 in renal tubular epithelial cells to reduce tubular epithelial mesenchymal transformation, prevent glomerular mesangial extracellular matrix protein accumulation and renal cell fibrosis, and protect DN.[45] These results suggest that miRNAs plays a key role in the occurrence and development of podocyte injury in DN and can be used as a potential biomarker. The study of the structure and function of miRNAs is a new and attractive target for the treatment of DN.

The enrichment results showed that glucose metabolic process, angiogenesis and negative regulation of transcription by RNA polymerase II were the most enriched BP items; extracellular exosome, plasma membrane and integral component of plasma membrane were the most enriched CC items; protein binding, protein homodimerization activity and metal ion binding were the most enriched MF items. Metabolic pathways, Hippo signaling pathways and protein digestion and absorption pathways are the top 3 significant pathways. These results demonstrate that DE miRNAs may function through these pathways and cell components. We have confirmed through experimental models that miR-103a-2-5p, miR-297, miR-548x-3p, miR-604, miR-644a, miR-1256, miR-3911 and miR-5047 can be used as biomarkers and molecular targets for the occurrence and development of diabetic nephropathy in this study. The 8 identified genes provide new insights into underlying molecular mechanisms of DN and can be utilized as promising therapeutic targets. Our research is of great significance for understanding the underlying mechanism of DN. The relationship between the identified miRNAs and DN has been verified through related molecular biology experiments. Since most of these miRNAs can be identified easily without the surgical approach, they can provide such a strong basis as therapeutic targets or potential biomarkers. Further studies are expected to verify the clinical application and explore optimal treatment strategies for DN.

Although this study has some limitations like is lack of experimental verification of core genes, we plan to do it immediately; also, the sample size is small, we can analyze more data sets or samples to further verify related targets in subsequent experiments, which helps us understand the occurrence and development of DN in more detail, and can also be analyzed together with molecular targets of other diseases to find clinical treatment methods that can be expanded. Moreover, further experiments are needed to examine the specific molecular mechanisms of diabetes nephropathy, these miRNAs-based treatments will be an option for the treatment of DN in the future.

Our study is just at the tip of the iceberg of understanding the prevention, diagnosis, treatment, and prognosis of DN. Further molecular biological experiments are necessary to confirm the function of the identified DEGs as well as the

interaction between microRNAs and genes in DN. In future studies, we also need to analyze more clinical samples to validate these results.

Data Sharing Statement

The data used to support the findings of this research are available from Gene Expression Omnibus database (https://www.ncbi.nlm.nih.gov/geo/);
miRBase database (http://www.mirbase.org/index.shtml);
miRDB database (http://mirdb.org/);
miRNAWalk database (http://mirwalk.umm.uni-heidelberg.de/);
TargetScan database (http://www.targetscan.org/mamm_31/);
RNA22 database (https://cm.jefferson.edu/rna22/Interactive/);
miRanda database (http://www.miranda.org/).

Ethics Statement

The Ethics Committee of the Third Affiliated Hospital of Soochow University approved this animal study. All animal experiments were conducted following the standard for laboratory animals of the Third Affiliated Hospital of Soochow University.

Author Contributions

All authors made a significant contribution to the work reported, whether that is in the conception, study design, execution, acquisition of data, analysis and interpretation, or in all these areas; took part in drafting, revising or critically reviewing the article; gave final approval of the version to be published; have agreed on the journal to which the article has been submitted; and agree to be accountable for all aspects of the work.

Disclosure

The authors report no conflicts of interest in this work.

References

1. Cho NH, Shaw JE, Karuranga S, et al. IDF diabetes atlas: global estimates of diabetes prevalence for 2017 and projections for 2045. *Diabetes Res Clin Pract*. 2018;138:271–281. doi:10.1016/j.diabres.2018.02.023
2. Fineberg D, Jandeleit-Dahm KA, Cooper ME. Diabetic nephropathy: diagnosis and treatment. *Nat Rev Endocrinol*. 2013;9(12):713–723. doi:10.1038/nrendo.2013.184
3. Bhattacharjee N, Barma S, Konwar N, Dewanjee S, Manna P. Mechanistic insight of diabetic nephropathy and its pharmacotherapeutic targets: an update. *Eur J Pharmacol*. 2016;791:8–24. doi:10.1016/j.ejphar.2016.08.022
4. Waijer SW, Sen T, Arnott C, et al. Association between tnf receptors and Kim-1 with kidney outcomes in early-stage diabetic kidney disease. *Clin J Am Soc Nephrol*. 2022;17(2):251–259. doi:10.2215/CJN.08780621
5. Ruggenenti P, Cravedi P, Remuzzi G. The raas in the pathogenesis and treatment of diabetic nephropathy. *Nat Rev Nephrol*. 2010;6(6):319–330. doi:10.1038/nrneph.2010.58
6. Cheng Y, Wang D, Wang F, et al. Endogenous mir-204 protects the kidney against chronic injury in hypertension and diabetes. *J Am Soc Nephrol*. 2020;31(7):1539–1554. doi:10.1681/ASN.2019101100
7. Bhat SA, Ahmad SM, Mumtaz PT, et al. Long non-coding RNAs: mechanism of action and functional utility. *Noncoding RNA Res*. 2016;1(1):43–50. doi:10.1016/j.ncrna.2016.11.002
8. Hosseinahli N, Aghapour M, Duijf PHG, Baradaran B. Treating cancer with microRNA replacement therapy: a literature review. *J Cell Physiol*. 2018;233(8):5574–5588. doi:10.1002/jcp.26514
9. Gholaminejad A, Abdul Tehrani H, Gholami Fesharaki M. Identification of candidate microRNA biomarkers in diabetic nephropathy: a meta-analysis of profiling studies. *J Nephrol*. 2018;31(6):813–831. doi:10.1007/s40620-018-0511-5
10. Dewanjee S, Bhattacharjee N. microRNA: a new generation therapeutic target in diabetic nephropathy. *Biochem Pharmacol*. 2018;155:32–47. doi:10.1016/j.bcp.2018.06.017
11. Conserva F, Barozzino M, Pesce F, et al. Urinary miRNA-27b-3p and miRNA-1228-3p correlate with the progression of kidney fibrosis in diabetic nephropathy. *Sci Rep*. 2019;9(1):11357. doi:10.1038/s41598-019-47778-1
12. Grayson PC, Eddy S, Taroni JN, et al. Metabolic pathways and immunometabolism in rare kidney diseases. *Ann Rheum Dis*. 2018;77(8):1226–1233. doi:10.1136/annrheumdis-2017-212935
13. Barrett T, Wilhite SE, Ledoux P, et al. NCBI geo: archive for functional genomics data sets–update. *Nucleic Acids Res*. 2013;41(Database issue):D991–D995. doi:10.1093/nar/gks1193

14. McDermaid A, Monier B, Zhao J, Liu B, Ma Q. Interpretation of differential gene expression results of RNA-seq data: review and integration. *Brief Bioinform*. 2019;20(6):2044–2054. doi:10.1093/bib/bby067
15. Kohl M, Wiese S, Warscheid B. Cytoscape: software for visualization and analysis of biological networks. *Methods Mol Biol*. 2011;696:291–303.
16. Livak KJ, Schmittgen TD. Analysis of relative gene expression data using real-time quantitative PCR and the 2 (-delta delta C(T)) method. *Methods*. 2001;25(4):402–408. doi:10.1006/meth.2001.1262
17. Lauber C, Correia N, Trumpp A, et al. Survival differences and associated molecular signatures of dnmt3a-mutant acute myeloid leukemia patients. *Sci Rep*. 2020;10(1):12761. doi:10.1038/s41598-020-69691-8
18. Guan H, Peng R, Fang F, et al. Tumor-associated macrophages promote prostate cancer progression via exosome-mediated mir-95 transfer. *J Cell Physiol*. 2020;235(12):9729–9742. doi:10.1002/jcp.29784
19. Geng Y, Zhao S, Jia Y, et al. Mir-95 promotes osteosarcoma growth by targeting scnn1a. *Oncol Rep*. 2020;43(5):1429–1436. doi:10.3892/or.2020.7514
20. Zhu H, Tang JH, Zhang SM, et al. Long noncoding RNA linc00963 promotes cdc5l-mediated malignant progression in gastric cancer. *Onco Targets Ther*. 2020;13:12999–13013. doi:10.2147/OTT.S274708
21. Li J, Huang S, Zhang Y, Zhuo W, Tong B, Cai F. Linc00460 enhances bladder carcinoma cell proliferation and migration by modulating mir-612/foxk1 axis. *Pharmacology*. 2020;105:1–12. doi:10.1159/000505216
22. Yu A, Zhao L, Kang Q, Li J, Chen K, Fu H. Transcription factor hif1α promotes proliferation, migration, and invasion of cholangiocarcinoma via long noncoding RNA h19/microRNA-612/bcl-2 axis. *Transl Res*. 2020;224:26–39. doi:10.1016/j.trsl.2020.05.010
23. Liu Y, Lu LL, Wen D, et al. Correction to: mir-612 regulates invadopodia of hepatocellular carcinoma by hadha-mediated lipid reprogramming. *J Hematol Oncol*. 2020;13(1):44. doi:10.1186/s13045-020-00875-5
24. Lin Y, Liu S, Su L, et al. Mir-570 inhibits proliferation, angiogenesis, and immune escape of hepatocellular carcinoma. *Cancer Biother Radiopharm*. 2018;33(6):252–257. doi:10.1089/cbr.2017.2389
25. Zhao H, Liu F, Jia R, et al. Mir-570 inhibits cell proliferation and glucose metabolism by targeting irs1 and irs2 in human chronic myelogenous leukemia. *Iran J Basic Med Sci*. 2017;20(5):481–488. doi:10.22038/IJBMS.2017.8671
26. Ren F, Shrestha C, Shi H, et al. Targeting of kdm5a by mir-421 in human ovarian cancer suppresses the progression of ovarian cancer cells. *Onco Targets Ther*. 2020;13:9419–9428. doi:10.2147/OTT.S266211
27. Huang B, Feng Z, Zhu L, et al. Silencing of microRNA-503 in rat mesenchymal stem cells exerts potent antitumorigenic effects in lung cancer cells. *Onco Targets Ther*. 2021;14:67–81. doi:10.2147/OTT.S282322
28. Cao X, Fan QL. Lncrna mir503hg promotes high-glucose-induced proximal tubular cell apoptosis by targeting mir-503-5p/bcl-2 pathway. *Diabetes Metab Syndr Obes*. 2020;13:4507–4517. doi:10.2147/DMSO.S277869
29. Perico L, Conti S, Benigni A, Remuzzi G. Podocyte-actin dynamics in health and disease. *Nat Rev Nephrol*. 2016;12(11):692–710. doi:10.1038/nrneph.2016.127
30. Wolf G, Chen S, Ziyadeh FN. From the periphery of the glomerular capillary wall toward the center of disease: podocyte injury comes of age in diabetic nephropathy. *Diabetes*. 2005;54(6):1626–1634. doi:10.2337/diabetes.54.6.1626
31. Wang X, Lin B, Nie L, Li P. microRNA-20b contributes to high glucose-induced podocyte apoptosis by targeting sirt7. *Mol Med Rep*. 2017;16(4):5667–5674. doi:10.3892/mmr.2017.7224
32. Zhong X, Chung AC, Chen HY, Meng XM, Lan HY. Smad3-mediated upregulation of mir-21 promotes renal fibrosis. *J Am Soc Nephrol*. 2011;22(9):1668–1681. doi:10.1681/ASN.2010111168
33. Loboda A, Sobczak M, Jozkowicz A, Dulak J. Tgf-beta1/smads and mir-21 in renal fibrosis and inflammation. *Mediators Inflamm*. 2016;2016:8319283. doi:10.1155/2016/8319283
34. Chen X, Zhao L, Xing Y, Lin B. Down-regulation of microRNA-21 reduces inflammation and podocyte apoptosis in diabetic nephropathy by relieving the repression of timp3 expression. *Biomed Pharmacother*. 2018;108:7–14. doi:10.1016/j.biopha.2018.09.007
35. Sakuma H, Hagiwara S, Kantharidis P, Gohda T, Suzuki Y. Potential targeting of renal fibrosis in diabetic kidney disease using microRNAs. *Front Pharmacol*. 2020;11:587689. doi:10.3389/fphar.2020.587689
36. McClelland AD, Herman-Edelstein M, Komers R, et al. miR-21 promotes renal fibrosis in diabetic nephropathy by targeting PTEN and SMAD7. *Clin Sci*. 2015;129(12):1237–1249. doi:10.1042/CS20150427
37. Zhao B, Li H, Liu J, et al. microRNA-23b targets ras GTPase-activating protein sh3 domain-binding protein 2 to alleviate fibrosis and albuminuria in diabetic nephropathy. *J Am Soc Nephrol*. 2016;27(9):2597–2608. doi:10.1681/ASN.2015030300
38. Zhou Z, Wan J, Hou X, Geng J, Li X, Bai X. microRNA-27a promotes podocyte injury via ppargamma-mediated beta-catenin activation in diabetic nephropathy. *Cell Death Dis*. 2017;8(3):e2658. doi:10.1038/cddis.2017.74
39. Qin W, Chung AC, Huang XR, et al. Tgf-beta/smad3 signaling promotes renal fibrosis by inhibiting mir-29. *J Am Soc Nephrol*. 2011;22(8):1462–1474. doi:10.1681/ASN.2010121308
40. Lin CL, Lee PH, Hsu YC, et al. microRNA-29a promotion of nephrin acetylation ameliorates hyperglycemia-induced podocyte dysfunction. *J Am Soc Nephrol*. 2014;25(8):1698–1709. doi:10.1681/ASN.2013050527
41. Xiao J, Meng XM, Huang XR, et al. Mir-29 inhibits bleomycin-induced pulmonary fibrosis in mice. *Mol Ther*. 2012;20(6):1251–1260. doi:10.1038/mt.2012.36
42. Kato M, Arce L, Wang M, Putta S, Lanting L, Natarajan R. A microRNA circuit mediates transforming growth factor-beta1 autoregulation in renal glomerular mesangial cells. *Kidney Int*. 2011;80(4):358–368. doi:10.1038/ki.2011.43
43. Yao T, Zha D, Gao P, Shui H, Wu X. Mir-874 alleviates renal injury and inflammatory response in diabetic nephropathy through targeting toll-like receptor-4. *J Cell Physiol*. 2018;234(1):871–879. doi:10.1002/jcp.26908
44. Zheng Z, Guan M, Jia Y, et al. The coordinated roles of miR-26a and miR-30c in regulating TGFβ1-induced epithelial-to-mesenchymal transition in diabetic nephropathy. *Sci Rep*. 2016;6:37492. doi:10.1038/srep37492
45. Huang Y, Tong J, He F, et al. Mir-141 regulates tgf-beta1-induced epithelial-mesenchymal transition through repression of hipk2 expression in renal tubular epithelial cells. *Int J Mol Med*. 2015;35(2):311–318. doi:10.3892/ijmm.2014.2008
46. Zhang Q, Sun W, Han J, et al. The circular RNA hsa_circ_0007623 acts as a sponge of microRNA-297 and promotes cardiac repair. *Biochem Biophys Res Commun*. 2020;523(4):993–1000. doi:10.1016/j.bbrc.2019.12.116

47. Xi X, Yao Y, Liu N, Li P. Mir-297 alleviates lps-induced a549 cell and mice lung injury via targeting cyclin dependent kinase 8. *Int Immunopharmacol*. 2020;80:106197. doi:10.1016/j.intimp.2020.106197
48. Zhang CZ. Long intergenic non-coding RNA 668 regulates vegfa signaling through inhibition of mir-297 in oral squamous cell carcinoma. *Biochem Biophys Res Commun*. 2017;489(4):404–412. doi:10.1016/j.bbrc.2017.05.155
49. Xu K, Liang X, Shen K, et al. Mir-297 modulates multidrug resistance in human colorectal carcinoma by down-regulating MRP-2. *Biochem J*. 2012;446(2):291–300. doi:10.1042/BJ20120386
50. Ramírez-Salazar EG, Almeraya EV, López-Perez TV, Patiño N, Salmeron J, Velázquez-Cruz R. microRNA-548-3p overexpression inhibits proliferation, migration and invasion in osteoblast-like cells by targeting stat1 and mafb. *J Biochem*. 2020;168(3):203–211. doi:10.1093/jb/mvaa033
51. Cheong JY, Shin HD, Cho SW, Kim YJ. Association of polymorphism in microRNA 604 with susceptibility to persistent hepatitis b virus infection and development of hepatocellular carcinoma. *J Korean Med Sci*. 2014;29(11):1523–1527. doi:10.3346/jkms.2014.29.11.1523
52. Wang X, He H, Rui W, Xie X, Wang D, Zhu Y. Long non-coding RNA bcar4 binds to mir-644a and targets tlx1 to promote the progression of bladder cancer. *Onco Targets Ther*. 2020;13:2483–2490. doi:10.2147/OTT.S232965
53. Liang W, Liao Y, Li Z, et al. microRNA-644a promotes apoptosis of hepatocellular carcinoma cells by downregulating the expression of heat shock factor 1. *Cell Commun Signal*. 2018;16(1):30. doi:10.1186/s12964-018-0244-z
54. Sahin Y, Altan Z, Arman K, Bozgeyik E, Koruk Ozer M, Arslan A. Inhibition of mir-664a interferes with the migration of osteosarcoma cells via modulation of meg3. *Biochem Biophys Res Commun*. 2017;490(3):1100–1105. doi:10.1016/j.bbrc.2017.06.174
55. Li Y, Yan X, Ren L, Li Y. Mir-644a inhibits cellular proliferation and invasion via suppression of ctbp1 in gastric cancer cells. *Oncol Res*. 2018;26 (1):1–8. doi:10.3727/096504016X14772410356982
56. Zhang JX, Chen ZH, Xu Y, et al. Downregulation of microRNA-644a promotes esophageal squamous cell carcinoma aggressiveness and stem cell-like phenotype via dysregulation of pitx2. *Clin Cancer Res*. 2017;23(1):298–310. doi:10.1158/1078-0432.CCR-16-0414
57. Wan D, Qu Y, Zhang L, Ai S, Cheng L. The lncrna linc00691 functions as a cerna for miRNA-1256 to suppress osteosarcoma by regulating the expression of st5. *Onco Targets Ther*. 2020;13:13171–13181. doi:10.2147/OTT.S266435
58. Wu C, Ma L, Wei H, Nie F, Ning J, Jiang T. Mir-1256 inhibits cell proliferation and cell cycle progression in papillary thyroid cancer by targeting 5-hydroxy tryptamine receptor 3a. *Hum Cell*. 2020;33(3):630–640. doi:10.1007/s13577-020-00325-x
59. Cai J, Chen Z, Wang J, et al. Circhectd1 facilitates glutaminolysis to promote gastric cancer progression by targeting mir-1256 and activating β-catenin/c-myc signaling. *Cell Death Dis*. 2019;10(8):576. doi:10.1038/s41419-019-1814-8
60. Wu L, Liu D, Yang Y. Enhanced expression of circular RNA circ-dcaf6 predicts adverse prognosis and promotes cell progression via sponging mir-1231 and mir-1256 in gastric cancer. *Exp Mol Pathol*. 2019;110:104273. doi:10.1016/j.yexmp.2019.104273
61. Chang H, Qu J, Wang J, Liang X, Sun W. Circular RNA circ_0026134 regulates non-small cell lung cancer cell proliferation and invasion via sponging mir-1256 and mir-1287. *Biomed Pharmacother*. 2019;112:108743. doi:10.1016/j.biopha.2019.108743
62. Liu W, Wan X, Mu Z, et al. Mir-1256 suppresses proliferation and migration of non-small cell lung cancer via regulating tctn1. *Oncol Lett*. 2018;16 (2):1708–1714. doi:10.3892/ol.2018.8794
63. Liu ZY, Yang L, Chang HY. Clinicopathologic and prognostic relevance of mir-1256 in colorectal cancer: a preliminary clinical study. *Eur Rev Med Pharmacol Sci*. 2018;22(22):7704–7709. doi:10.26355/eurrev_201811_16391
64. Li Y, Kong D, Ahmad A, Bao B, Dyson G, Sarkar FH. Epigenetic deregulation of mir-29a and mir-1256 by isoflavone contributes to the inhibition of prostate cancer cell growth and invasion. *Epigenetics*. 2012;7(8):940–949. doi:10.4161/epi.21236
65. He T, Sun R, Li Y, Katusic ZS. Effects of brain-derived neurotrophic factor on microRNA expression profile in human endothelial progenitor cells. *Cell Transplant*. 2018;27(6):1005–1009. doi:10.1177/0963689718761658
66. Kocyigit I, Taheri S, Sener EF, et al. Serum RNA profiles in patients with autosomal dominant polycystic kidney disease according to hypertension and renal function. *BMC Nephrol*. 2017;18(1):179. doi:10.1186/s12882-017-0600-z
67. Sun Q, Zhang Y, Wang S, et al. Neat1 decreasing suppresses Parkinson's disease progression via acting as mir-1301-3p sponge. *J Mol Neurosci*. 2021;71(2):369–378. doi:10.1007/s12031-020-01660-2
68. Chen C, Jiang L, Zhang Y, Zheng W. Foxa1-induced linc01207 facilitates head and neck squamous cell carcinoma via up-regulation of tnrc6b. *Biomed Pharmacother*. 2020;128:110220. doi:10.1016/j.biopha.2020.110220
69. Guo J, Chen M, Ai G, Mao W, Li H, Zhou J. Hsa_circ_0023404 enhances cervical cancer metastasis and chemoresistance through vegfa and autophagy signaling by sponging mir-5047. *Biomed Pharmacother*. 2019;115:108957. doi:10.1016/j.biopha.2019.108957